DYNAMO: Dynamic Multi-Model Source Localization Method for EEG and/or MEG

Javier M. Antelis and Javier Minguez

Abstract— **This paper proposes a multiple model method that addresses the estimation of the EEG/MEG neural sources as a multihypothesis, multidimensional and dynamic estimation problem. The key aspect is the probabilistic integration of several neural models to simultaneously estimate and integrate the brain activity of different dynamic neural processes that are characterized by the number of sources, the dynamic of those sources and the initial conditions. The method was validated with EEG data gathered in a protocol to elicit error-related potentials, since there is evidence of the brain region that generate those signals. The results reveal that the proposed multiple model method is able to identify the brain structure associated with error processing, which is a preliminary indicator of the validity of the proposed method.**

I. INTRODUCTION

Electroencephalography (EEG) and magnetoencephalography (MEG) are non-invasive techniques that measure the electrical activity of neurons in the brain with high temporal resolution. However, interpretation of EEG and MEG signals entails speculation of the brain active areas that generate those signals. This leads to the EEG/MEG source localization problem: to estimate the neural sources that generate the EEG/MEG signals. This is an ill-posed problem since there are infinite configurations of neural sources that consistently could produce the EEG and MEG observations [1]. In addition, depending on the cognitive tasks, the number of brain active areas and their associated temporal dynamic are continually changing. Therefore, the estimation of the EEG/MEG neural sources could be seen as a multihypothesis, multidimensional and dynamic estimation problem.

This paper proposes the *Dynamo* method, a multi-model solution for the EEG/MEG source localization problem that relies on the integration of many dynamic dipolar neural models explaining multiple hypothesis of the brain activity. A neural model is defined as an input-state-output dynamic system that is characterized by the number of sources and the underlying dynamic of those sources, which allows to estimate a neural process within a recursive filter estimation framework [2]. The underlying idea in the proposed multiple model method is to assemble a bank of filters to simultaneously estimate and integrate the brain activity of different dynamic dipolar neural processes. This provides two key characteristics. First, the estimation of the neural sources is the probabilistic fusion of many available hypotheses. Second, the simultaneous consideration of many different neural models provides a straightforward way to deal with the multidimensionality and the different dynamics of the neural sources.

The method was validated with real EEG signals gathered during the execution of an experimental protocol designed to elicit error-related potentials, since there is evidence of the brain region responsible for the generation of those potentials [3], [4]. The results demonstrated that the method was able to successfully localize the brain region associated with error processing, which is a preliminary indicator of the validity of the proposed method.

J.M. Antelis and J. Minguez are with the Aragon Institute of Engineering Research (I3A) and Department of informatics and Systems Engineering, University of Zaragoza, 50018 Zaragoza, Spain. antelis@unizar.es, jminguez@unizar.es

This work has been partly supported by the Spanish projects HYPER-CSD2009- 00067, DPI2009-14732-C02-01 and by grants of Santader Bank and University of Zaragoza

II. DYNAMIC MULTIPLE MODEL ESTIMATION OF THE EEG/MEG NEURAL SOURCES

Let the EEG and MEG measurements at time t be $\Phi_t = [\phi_t^1 ... \phi_t^{N_\phi}]^T$ and $\mathbf{b}_t = [b_t^1 ... b_t^{N_b}]^T$. Let the measurement vector be $\mathbf{m}_t = [\Phi_t, \mathbf{b}_t]^T$. Lets assume N_s dipolar sources in the brain, which are characterized by the position $\mathbf{r}_q \in \Re^3$ and moment $\mathbf{q} \in \Re^3$. The sources state is $\mathbf{x}_t = [\mathbf{r}_q^1, \mathbf{q}^1 \dots \mathbf{r}_q^{N_s}, \mathbf{q}^{N_s}]^T$, $\mathbf{x} \in \Re^{6 \cdot N_s}$. The goal is to recursively estimate $\mathbf{x}_t$ and its associated covariance $\mathbf{P}_t$ given new measurements $\mathbf{m}_t$. There are two physical systems involved to solve this problem: *(i)* a state transition model which is the linear random walk function with a zero-mean Gaussian noise, and *(ii)* the measurement model which is linear with respect to the moment but non-linear with respect to the position and with a zero-mean Gaussian noise. For this nonlinear and Gaussian system, the recursive estimation of the neural sources leads to the Extended Kalman Filter (EKF). Figure 1a shows a graphical representation of the execution of the EKF algorithm for the estimation of the EEG/MEG neural sources, which was introduced in [5]. The intrinsic limitations of this framework are: *(i)* The number of neural sources is fixed. *(ii)* A unique neural dynamic is taken into account. *(iii)* The selection of the prior estimate of the brain activity is fixed. In fact, these are the shortcomings to address the present problem since it is multi-hypothesis, multidimensional and with time-varying dynamic.

This paper addresses all these limitations in an unified framework by the probabilistic integration of multiple neural models. The method is illustrated in Figure 1b. The core idea is a bank of r EKF filters (where $\{\mathbf{x}, \mathbf{P}\}_{t|t}^i$ is the sources state and the covariance for the i-th filter) executed in parallel estimating neural models with different number of sources, dynamics and initial conditions, which represent different

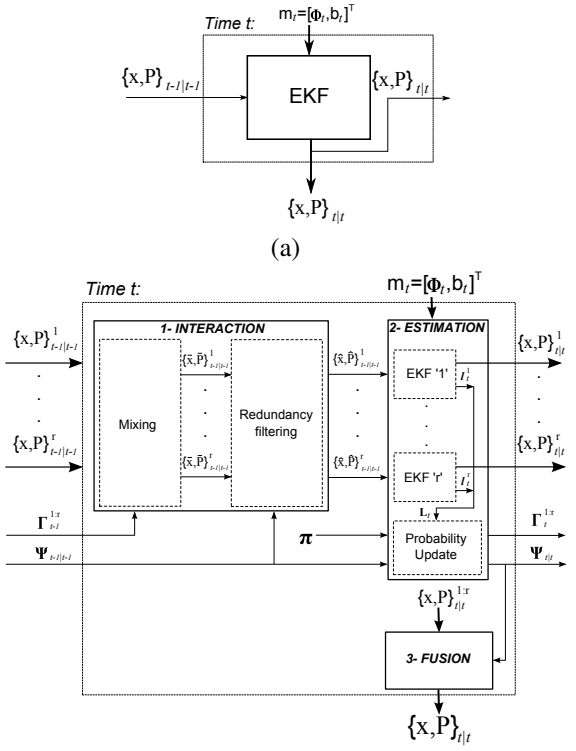

Fig. 1. (a) EKF estimation framework for a single neural model. (b) Graphical representation of the Multiple Model Estimation framework.

hypotheses of the brain activity. The algorithm is executed in three steps, (i) Interaction, (ii) Estimation, and (iii) Fusion.

A. Interaction Step

The objective in this step is to probabilistically mix prior estimates to combine the information of all the filters (Mixing), and to disjoin estimations that are explaining the same hypothesis of the brain activity (Redundancy filtering).

1) Mixing: The prior mixed estimate for the i-th filter is computed as a weighted combination of the prior estimates given by all the filters:

$$\overline{\mathbf{x}}^i_{t-1|t-1} = \sum_{j=1}^{r} \mathbf{x}^j_{t-1|t-1} \gamma^{j|i}_{t-1} \tag{1}$$

$$\begin{aligned} \overline{\mathbf{P}}^i_{t-1|t-1} = \; & \sum_{j=1}^{r} \Big[\mathbf{P}^j_{t-1|t-1} + \\ & \left(\overline{\mathbf{x}}^i_{t-1|t-1} - \mathbf{x}^j_{t-1|t-1}\right) \cdot \\ & \left(\overline{\mathbf{x}}^i_{t-1|t-1} - \mathbf{x}^j_{t-1|t-1}\right)^T \Big] \gamma^{j|i}_{t-1} \end{aligned} \tag{2}$$

where $\Gamma^i_{t-1} = [\gamma^{1|i}_{t-1}, \cdots, \gamma^{r|i}_{t-1}]$ is the mixing probability vector for filter i which is defined in the previous estimation step.

2) Redundancy Filtering: This is a random process that re-initialize those filters that are estimating statistically similar hypothesis of the brain activity. Lets consider the set of prior mixed estimates $\left\{\overline{\mathbf{x}}, \overline{\mathbf{P}}\right\}^{1:r}_{t-1|t-1}$. The Mahalanobis distance between two of those estimations is defined as:

$$\begin{aligned} d^2_{m|n} = \; & \left(\overline{\mathbf{x}}^m_{t-1|t-1} - \overline{\mathbf{x}}^n_{t-1|t-1}\right)^T \cdot \\ & \left(\overline{\mathbf{P}}^m_{t-1|t-1} + \overline{\mathbf{P}}^n_{t-1|t-1}\right)^{-1} \cdot \\ & \left(\overline{\mathbf{x}}^m_{t-1|t-1} - \overline{\mathbf{x}}^n_{t-1|t-1}\right) \end{aligned} \tag{3}$$

where $m = 1, \cdots, r$ and $n = 1, \cdots, r$ with $m \neq n$. In the case that $d^2_{m|n}$ is lower than the inverse χ^2 cumulative distribution function up to a significance level, then, both estimates are explaining statistically similar hypothesis. Therefore, a random process re-initialize the filter with the lower probability, e.g.:

$$\widehat{\mathbf{x}}^n_{t-1|t-1} \sim \mathcal{N}(0, \mathbf{P}_0) \quad ; \quad \widehat{\mathbf{P}}^n_{t-1|t-1} = \mathbf{P}_0 \tag{4}$$

where $\mathbf{P}_0$ is a diagonal matrix whose elements are defined to cover the brain, ensuring that the prior estimate falls within the brain volume. Otherwise, both prior mixed estimates are explaining different hypothesis.

B. Estimation Step

In this step the EKF filters run independently producing their own estimation of the neural sources $\{\mathbf{x}, \mathbf{P}\}^i_{t|t}$ from the prior estimate and the new available EEG/MEG measurements $\mathbf{m}_t$. In addition, the belief of the estimation given by each filter and the mixing probability are computed. On the one hand, the belief of the bank of filters is represented as a state vector of posterior probabilities $\Psi_{t|t} = [\psi^1_{t|t}, \cdots, \psi^r_{t|t}]^T$, which are normalized $\sum_{i=1}^{r} \psi^i_{t|t} = 1$. This state vector of probabilities is recursively updated as:

$$\Psi_{t|t} = \mathbf{L}_t \Psi^T_{t|t-1} \tag{5}$$

where $\mathbf{L}_t = [l^1_t, \cdots, l^r_t]^T$ and $l^i_t = p(\mathbf{m}_t|\mathbf{x}^i_{t|t})$ is the likelihood function of the data given that the estimation of the filter i is correct, which follows a normal distribution since the measurement noise is Gaussian. Furthermore, $\Psi_{t|t-1} = [\psi^1_{t|t-1}, \cdots, \psi^r_{t|t-1}]^T$ is the predicted probability vector defined as $\Psi_{t|t-1} = \pi \Psi_{t-1|t-1}$, where $\Psi_{t-1|t-1} = [\psi^1_{t-1|t-1}, \cdots, \psi^r_{t-1|t-1}]^T$ is the prior probability state vector and π is a transition probability matrix kernel that follows a homogeneous constant Markov process. The entry π_{ji} represents the probability that at time t the selected filter is i given that at time $t-1$ the selected filter had been j [6].

On the other hand, the mixing probability vector for filter i is computed as:

$$\gamma^{j|i}_t = \frac{\pi_{ji} \psi^j_{t-1|t-1}}{\psi^i_{t|t-1}} \quad , \quad \forall\, j = 1, ..., r \tag{6}$$

which is used the next time instant in the interaction step.

C. Estimate Fusion

In this step, the multiple hypotheses are combined:

$$\mathbf{x}_{t|t} = \sum_{i=1}^{r} \mathbf{x}^i_{t|t} \psi^i_{t|t} \tag{7}$$

$$\mathbf{P}_{t|t} = \sum_{i=1}^{r} \left[\mathbf{P}^i_{t|t} + \left(\mathbf{x}_{t|t} - \mathbf{x}^i_{t|t}\right) \left(\mathbf{x}_{t|t} - \mathbf{x}^i_{t|t}\right)^T \right] \psi^i_{t|t} \tag{8}$$

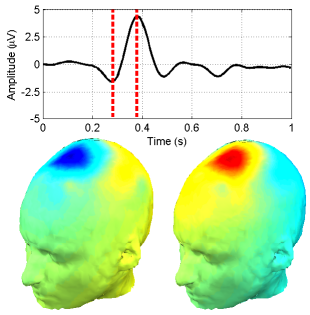

Fig. 2. Grand difference averaged for all the subjects at channel FCz and topography scalp maps in the EEG distribution at times 281 and 379 ms.

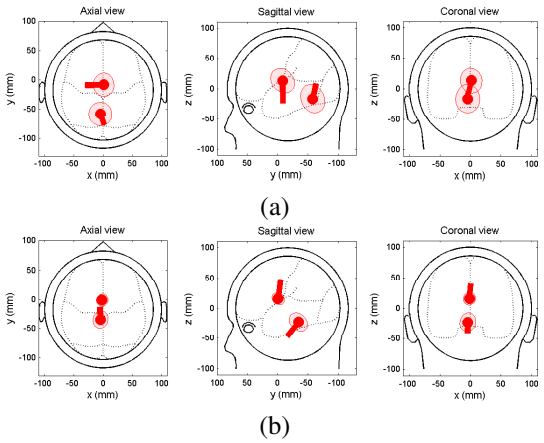

Fig. 3. Neural sources estimated with the proposed multiple model method. (a) At time 281 ms. (b) At time 379 ms.

Notice that the final estimation $\{\mathbf{x}, \mathbf{P}\}_{t|t}$ is a weighted fusion in terms of probabilities of the multiple hypotheses given by the filters.

III. EXPERIMENTAL VALIDATION

A. Experimental protocol, instrumentation and implementation of the method

In order to assess the performance of the proposed method, it was designed a neurophysiological protocol to evoke feedback error-related potentials (ErrP), since there is evidence indicating that the main focus of neural activity is expected to be mainly in the anterior cingulate cortex (ACC) [3]. The feedback stimuli time-estimation protocol was followed [4]. The mental task was to estimate the duration of one second. The subject indicates by pressing a button the end of the time interval, and he/she receives a visual feedback that indicates whether the estimated interval was correct or incorrect. A visual feedback indicating incorrect performance elicits a negative and next a positive peak that are measured mainly in the electrodes situated over the midline, whose measurements are much smaller if the visual feedback indicates correct performance [7].

Five healthy male subjects participated in the experimental sessions. For each participant 150 error trials and 150 correct trials were evoked. EEG activity was recorded from 32 electrodes arranged according to the 10/10 international system. The ground electrode was positioned on the forehead and the reference electrode was placed on the left earlobe. The EEG was amplified, digitized with a sampling frequency of 256Hz, power-line notch-filtered and bandpass-filtered between 0.5 and 60Hz. After the experimental sessions, the EEG signals were average referenced and a time window of one second was selected after the visual feedback stimulus onset. All error and correct trials were then low pass filtered to 10Hz with no phase shift. See [8] for further details.

The head was modeled by three-shell concentric spheres. Radiuses were fixed to 86, 96 and 100mm and conductivities were fixed to 0.33 S/m for brain and scalp and 0.0042 S/m for skull. The head model, the sources position and the electrodes locations were defined in the coordinate system of the realistic MNI head model. The multiple model method was implemented with neural models of 1, 2 and 3 dipolar sources (as stated in other studies, a maximum number of three dipolar sources is sufficient to explain focalized brain activations [9]) with 4, 8 and 16 EKF filters respectively.

B. Analysis and Results

The neural sources of the grand difference averaged for all the subjects and for each subject individually were estimated using the proposed method.

1) Neurophysiological process validation: The first objective was to determine whether feedback ErrP's were elicited. Figure 2 shows the grand average difference between error and correct trials averaged for all the subjects at channel FCz. The waveform reveals a negative deflexion at 281 ms and a positive peak at 379 ms after the presentation of the feedback, which indicates strong differences between error and correct trials. These results point out that feedback ErrP's are elicited after the visual stimulus presentation. This figure also shows the topography scalp maps at the occurrence of these two peaks revealing focused fronto-central activity. This result seems to indicate that the main focus of neural activity is in a frontal-central structure of the brain, which agrees with the results reported in [3] and [4].

2) Neural sources estimation: The neural sources responsible for the generation of the grand average difference potentials averaged for all the subjects were estimated with the proposed method. Figure 3 shows the neural sources estimated during the occurrence of the negative and positive peaks showed above in figure 2. In both peaks two focus of neural activity were estimated. One of the sources is estimated in Brodmann area 24 that represents the anterior cingulate. The estimation of this source is consistent with previous studies of feedback ErrP's [4]. Hence, these results give evidence that Dynamo correctly estimates the focalized brain active area associated with error processing. Further, note also that in both peaks the additional source is estimated in the deep brain (which also agrees with the results reported in [4]), for the first negative peak in the occipital lobe (visual processing center) and for the second positive peak in the parahippocampal gyrus (associated with the encoding

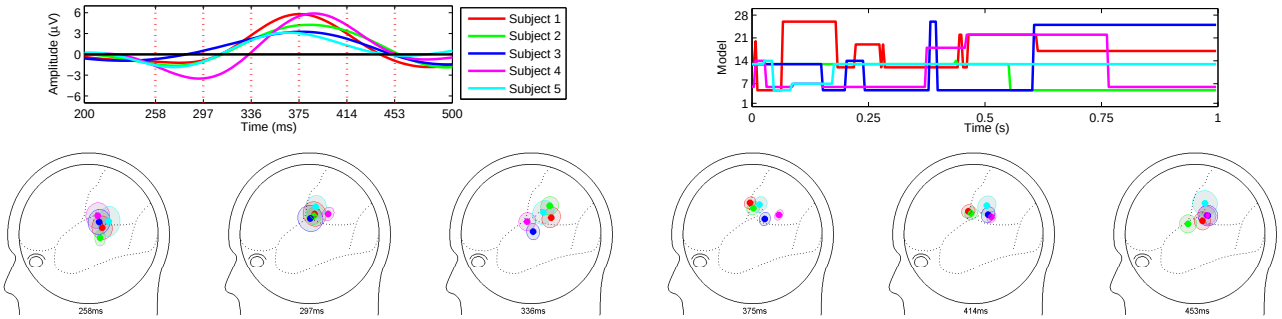

Fig. 4. Right top: waveforms of the grand average difference for all the subjects at channel FCz. Left top: number of the model with the highest probability for all the subjects. Bottom: one of the estimated sources for all the subjects at some predefined time instants.

and recognition of scenes), which might suggest the mental process related with the recognition of the visual feedback cues. Importantly, although it have been stated that a single dipole is sufficient to explain the focalized neural activity underlying error processing [10], the estimation given by the method could suggest that an additional neural system is also active. This highlights one important characteristic of the method, the number of sources is automatically estimated allowing the estimations of several brain active areas.

3) Neural sources estimation across subjects: Figure 4 shows for all the subjects: *(i)* the waveforms of the grand average difference at channel FCz (left top), *(ii)* one of the estimated neural sources at predefined time instants (bottom), and *(iii)* the model with the highest posterior probability (right top). On the first hand, the estimated neural sources for all the subjects are located quite similar, which indicates the high robustness of the method across subjects. On the second hand, the covariances are smaller at time instants when the signals have large magnitude (e.g. 375 ms), although not shown here in such cases the scalp distribution is highly focalized. Nonetheless, the covariances are greater at time instants when the signals have a small magnitude, in such cases the scalp distribution is widespread (e.g. 258 ms). This result point out an additional characteristic of the method that is not available in traditional dipolar approaches: for those cases when the brain activity is presumably distributed, the uncertainty about the dipolar estimation increases revealing that the interpretation of the brain active areas should be taken with care. Finally, notice that for all the subjects the model with the highest probability is changing along the time, which indicates that models with different parameters (e.g number of sources) are being selected. This result explicitly shows the multi-model operation that highlights the core of the method.

IV. CONCLUSIONS

This work describes a multi-model solution for the EEG/MEG source localization problem that relies on the integration of many dynamic dipolar neural models. This provides several characteristics, *(i)* the consideration of different models allows to estimate various hypotheses of brain activity (multihypothesis), *(ii)* a straightforward way to deal with the natural changes in the number of active brain areas (multidimensionality), *(iii)* the consideration of time-varying dynamic in the neural sources (neural dynamic), and *(iv)* a straightforward way to initialize the filters (multiple prior estimates). Unlike some dipolar methods, this approach does not to make prior assumptions about the number of active sources. Furthermore, the method also automatically computes the uncertainty matrix of the neural sources allowing to infer whether those estimated sources are highly focalized or not. The performance of the method was validated in real settings with feedback ErrP's. On the basis of the experimental results, the method was able to successfully identify not only the brain region underlying error processing, but also brain regions related with the recognition and processing of the visual feedback cues, which are activated during the execution of the mental task.

REFERENCES

[1] S. Baillet, J. Mosher, and R. Leahy, "Electromagnetic brain mapping," *IEEE Signal Processing Magazine*, vol. 18, pp. 14–30, 2001.

[2] J. M. Antelis and J. Minguez, "Dynamic solution to the EEG source localization problem using kalman filters and particle filters," in *31st Annual International Conference of the IEEE Engineering in Medicine and Biology Society (EMBC)*, Minneapolis, USA, 2009.

[3] H. T. van Schie, R. B. Mars, M. G. H. Coles, and H. Bekkering, "Modulation of activity in medial frontal and motor cortices during error observation," *Nature Neuroscience*, vol. 7, pp. 549–554, 2004.

[4] W. H. Miltner, C. H. Braun, and M. G. H. Coles, "Event-related brain potentials following incorrect feedback in a time-estimation task: Evidence for a generic neural system for error detection," *Journal of Cognitive Neuroscience*, vol. 9, pp. 788–798, 1997.

[5] J. M. Antelis and J. Minguez, "EEG source localization based on dynamic bayesian estimation techniques," *International Journal of Bioelectromagnetism*, vol. 11(4), pp. 179–184, 2009.

[6] Y. Bar-Shalom, X. R. Li, and T. Kirubarajan, *Estimation with Applications to Tracking and Navigation: Theory, Algorithms and Software*. Wiley, 2001.

[7] C. B. Holroyd and M. G. Coles, "The neural basis of human error processing: reinforcement learning, dopamine, and the error-related negativity." *Psychol Rev*, vol. 109, no. 4, pp. 679–709, October 2002.

[8] E. Lopez-Larraz, I. Iturrate, L. Montesano, and J. Minguez, "Real-time recognition of feedback error-related potentials during a time-estimation task," in *32nd Annual International Conference of the IEEE Engineering in Medicine and Biology Society (EMBS)*, Buenos Aires, Argentina, 2010.

[9] C. Plummer, A. S. Harvey, and M. Cook, "EEG source localization in focal epilepsy: Where are we now?" *Epilepsia*, vol. 49, no. 2, pp. 201–2018, 2008.

[10] S. Dehaene, M. I. Posner, and D. M. Tucker, "Localization of neural system for error detection and compensation," *Psychological Science, American Psychological Society*, vol. 5(5), pp. 303–305, 1994.